

Biexciton kinetics in GaN quantum wells: Time-resolved and time-integrated photoluminescence measurements

Flavian Stokker Cheregi,¹ Anna Vinattieri,¹ Eric Feltin,² Dobri Simeonov,² Jean-François Carlin,² Raphaël Butté,² Nicolas Grandjean,² and Massimo Gurioli¹

¹*Department of Physics and LENS, Università di Firenze, 50019 Sesto Fiorentino, Italy*

²*Institute of Quantum Electronics and Photonics, Ecole Polytechnique Fédérale de Lausanne, CH-1015 Lausanne, Switzerland*

(Received 9 October 2007; published 28 March 2008)

We report on the experimental achievement of narrow ultraviolet excitonic and biexcitonic emission from GaN/AlGaIn quantum wells. The very large biexciton binding energy (up to 12 meV) inhibits thermalization between the two species allowing to study the recombination kinetics of the biexciton gas. By performing resonant and nonresonant time resolved measurements, we elucidate the interplay between biexciton formation and exciton acoustic-phonon mediated relaxation within localized states.

DOI: [10.1103/PhysRevB.77.125342](https://doi.org/10.1103/PhysRevB.77.125342)

PACS number(s): 78.47.-p, 78.55.Cr, 71.35.-y

The exciton, an electron-hole pair bound by the attractive Coulomb force, is the fundamental optical transition of a semiconductor system or nanostructure. At the same time, the exciton is a free particle which, similar to atoms in gas phase, may interact to produce exciton molecules (biexcitons). A relevant requirement for the observation of the biexciton formation in a semiconductor quantum well (QW) is the high optical quality of the nanostructures. The in-plane structural disorder produces exciton localization (which strongly reduces the probability of biexciton formation) and it determines the inhomogeneous broadening of the exciton optical resonance (which may mask the biexciton recombination). Indeed, one of the most relevant signatures for assessing the optical quality of QWs is the presence of biexciton recombination. For these reasons, a lot of studies on biexciton properties in III-V semiconductors have been performed in GaAs based QWs,¹⁻³ where the optical quality is nowadays extremely high. However, a relevant drawback of GaAs QWs is that the biexciton binding energy is in the range of 1 meV. As a consequence, the biexciton gas thermalizes with the excitons resulting in a common averaged kinetics.³ In ionic II-VI QWs, the biexciton energy increases up to about 10 meV and stable biexcitons are observed. These are found to play a key role in the stimulated emission process.⁴ Despite this, little work has been dedicated to the biexciton kinetics in II-VI QWs,^{5,6} also because often the large inhomogeneous broadening tends to mix exciton and biexciton emissions.⁵ Moreover, II-VI materials have been nowadays largely outstripped by nitrides as reliable wide band gap semiconductors, e.g., for optoelectronic devices.

Nitride-based QWs offer the advantage of large Coulomb interaction, with an exciton binding energy estimated to be larger than 30 meV in low Al content narrow GaN/AlGaIn QWs.⁷ Consequently, exciton and biexciton effects could be potentially exploited for realizing a novel class of nitride-based devices. Presently, GaN based nanostructures are already the basis of large classes of blue and ultraviolet optoelectronic devices.⁸ Although these devices exhibit impressive performances, in depth physical studies have been hindered by the optical quality of nitride heterostructures which is still far from being ideal. The lattice mismatch between standard substrates and heteroepitaxially grown ma-

terials produces structural defects with a density 6 orders of magnitude larger than in conventional GaAs based structures.⁹ Correspondingly, the concentration of non radiative centers is non-negligible,¹⁰ thus reducing the recombination lifetime. Large inhomogeneous broadening of the optical spectra is also usually observed as a consequence of strain, interface, and alloy fluctuations.¹¹ Finally, the quantum confined Stark effect associated with the huge piezo and spontaneous polarization fields reduces the radiative recombination rate and eventually may even inhibit the excitonic recombination.¹²

In this paper, we report the achievement of high quality GaN/AlGaIn QWs with strong excitonic recombination and inhomogeneous broadening (Stokes shift) as small as 5 meV (3.6 meV). Evidence for biexciton recombination is found when increasing the excitation intensity. Very large biexciton binding energy, up to 12 meV, has been observed, confirming the strong Coulomb interaction in III-nitride QWs. This peculiarity strongly modifies the exciton—biexciton recombination kinetics with respect to GaAs based QWs, allowing us to probe the thermodynamics between excitons and biexcitons and to investigate the biexciton formation and recombination dynamics. By performing resonant and nonresonant time resolved measurements, we thus elucidate the interplay between exciton relaxation within localized states and biexciton formation.

The samples were grown by metal organic vapor phase epitaxy on *c*-plane sapphire substrates. The templates are composed of a standard 3 μm GaN buffer layer and a 200 nm thick $\text{Al}_x\text{Ga}_{1-x}\text{N}$ layer. Single GaN QWs with a thickness of 2.6 nm were then deposited and capped with a 50 nm thick $\text{Al}_x\text{Ga}_{1-x}\text{N}$ layer (with $x=5\%$ or $x=9\%$). Details on the growth and on the interface structure can be found in Ref. 13. Time-resolved (TR) and time-integrated (TI) photoluminescence (PL) measurements were performed by using the second and third harmonic generations of a mode-locked Ti:sapphire laser, pumped by a cw Ar^+ laser, providing 1.2 ps pulses with a repetition rate of 81 MHz. The excitation density was changed in the range of 0.2–20 W/cm^2 . The samples were kept in a closed cycle cryostat and the PL was detected by a streak camera apparatus with an experimental time resolution of 3 ps and a spectral resolution of 1 meV.

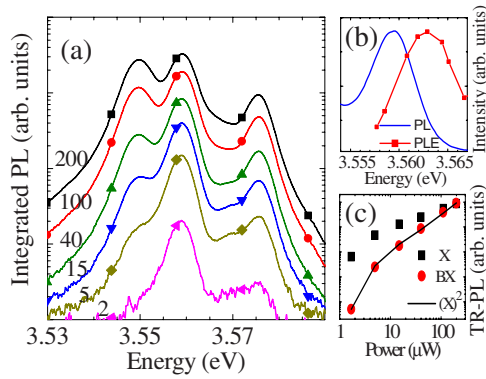


FIG. 1. (Color online) (a) TI-PL spectra of the 2.6 nm thick GaN/Al_{0.05}Ga_{0.95}N QW measured at 10 K for different excitation power densities in semilogarithmic scale (the excitation powers in microwatts are reported in the figure). (b) Comparison between PL and PLE spectra measured at 10 K. (c) Comparison of the X and BX TR-PL intensities in logarithmic scale. The line is the square of the X TR-PL intensity scaled in order to fit with the BX data.

Figure 1(a) shows, in semilogarithmic scale, the TI-PL spectra measured at 10 K of the 2.6 nm thick GaN/Al_{0.05}Ga_{0.95}N QW for different excitation power densities. The peak at 3.575 eV corresponds to the recombination from the Al_{0.05}Ga_{0.95}N barrier and the peak at 3.559 eV is the excitonic recombination (X) from the GaN QW, showing an overall broadening as small as 5 meV. We report in Fig. 1(b) the comparison between TI-PL and PL excitation (PLE) spectra measured at 10 K, denoting a Stokes shift of only 3.6 meV. When increasing the pump intensity, a peak at about 9 meV below the exciton peak grows superlinearly with the excitation power. This trend is not consistent with bound exciton recombination—in agreement with the low impurity content, the estimated *n*-type background doping being as low as 10¹⁶ cm⁻³—which should instead saturate at high excitation. The PL superlinearity is the fingerprint of biexciton recombination (BX), whose density is predicted to scale quadratically with the exciton population. In order to carefully analyze this point, in Fig. 1(c), we compare the initial exciton and biexciton populations, as obtained from the emission intensity of TR-PL spectra with a time window of 70 ps (see also Fig. 3) at the PL peak. As expected,² the exciton recombination exhibits a sublinear increase with increasing excitation power density, while the biexciton perfectly follows the law $BX \propto X^2$. Note that a biexciton binding energy up to 12 meV has been measured in the 2.6 nm thick GaN/Al_{0.09}Ga_{0.91}N QW (not reported here). The huge biexciton binding energy very likely reflects both the strong Coulomb interaction in nitrides and, to a lesser extent, the enhancement of the Haynes factor associated with localization due to structural disorder.¹⁴

Let us now address the interplay between biexciton formation and ionization by means of PL spectra taken at different temperatures. TI-PL data are shown in Fig. 2. Very small changes are found between 10 and 20 K, both for X and BX. At 30 K, the X emission intensity is only slightly decreased, while the emission at the BX is already reduced, and for higher temperatures (*T*), the exciton emission also starts to quench. As a matter of fact, a thermodynamic and

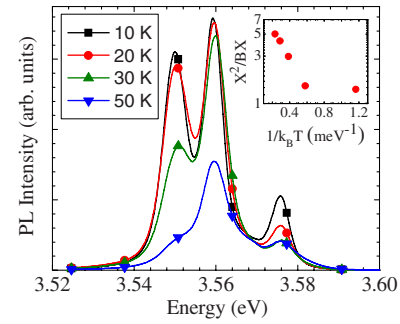


FIG. 2. (Color online) TI-PL spectra of the 2.6 nm thick GaN/Al_{0.05}Ga_{0.95}N QW measured at different temperatures for a power density of 20 W/cm² in a linear scale. Inset: semilogarithmic plot of the ratio between the square of the integrated PL intensity at the X band divided by the BX integrated PL intensity as a function of $1/k_B T$.

chemical equilibria between X and BX have been observed in GaAs QWs,³ due to the very fast thermalization process as compared with the recombination one. This leads to a mass action law $n_X^2/n_{BX} \propto \exp(-\Delta_{BX}/k_B T)$, where Δ_{BX} is the BX binding energy and n_X and n_{BX} are the exciton and biexciton densities, respectively.³ The 9 meV biexciton binding energy, to be compared with 1.5 meV in GaAs QWs,² suggests a much longer time for the biexciton dissociation at low *T* in GaN QWs, and therefore a different interplay between X and BX is expected. The semilogarithmic plot of the ratio between the square of the integrated PL intensity at the X band divided by the BX integrated PL intensity is reported as a function of $1/k_B T$ in the inset of Fig. 2. Clearly, the BX and X populations are not thermalized at low *T*, and eventually, the biexciton ionization starts to play a role, throughout the exciton lifetime, only for $T \geq 30$ K. Therefore, we can use TR-PL data measured at *T*=10 K to determine the rates for the formation and recombination of the X and BX bands.

The image of the TR-PL measured under nonresonant excitation (at 267 nm, that is, more than 1 eV above the QW exciton transition) is shown in Fig. 3(a), as measured by the streak camera apparatus. The TR-PL spectra, obtained by horizontal cuts of the streak image at different time steps, are reported in Fig. 3(b), showing an energy shift of the X line of approximately 1 meV in the initial dynamics. Note that the observed shift does not depend on the excitation power and therefore it cannot be attributed to the screening of the piezoelectric field. This is consistent with the estimated carrier density ($\sim 2.5 \times 10^{11}$ cm⁻²) at the highest excitation power used, which is well below that where screening effects are expected to occur.¹⁵ As discussed below, we attribute this shift to acoustic-phonon mediated relaxation between excitonic localized states.

In addition, the X and BX emissions follow different recombination kinetics. This is further elucidated by the time evolution of the X and BX emissions, reported in Fig. 3(c). Clearly, the BX band shows a longer rise time and a faster decay time as compared to the excitonic emission. In Fig. 3(c), the square of the excitonic emission is reported for comparison. This trend is expected for the BX time evolution on the basis of thermodynamic equilibrium between X and

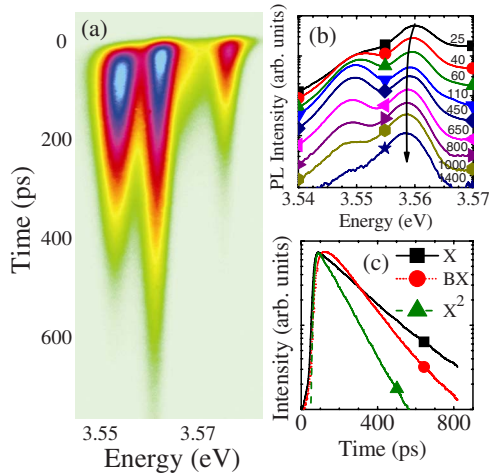


FIG. 3. (Color online) (a) Image of the TR-PL of the 2.6 nm thick GaN/ $\text{Al}_{0.05}\text{Ga}_{0.95}\text{N}$ QW measured at $T=10$ K and at a power density of 20 W/cm^2 under nonresonant excitation at 267 nm, as measured by the streak camera apparatus. (b) TR-PL spectra at different time delays with time steps reported in picoseconds, in semilogarithmic scale. The line is a guide to the eye. (c) Decays of the exciton and biexciton emissions in semilogarithmic scale. The square of the excitonic emission is also reported for comparison.

BX, an aspect already observed in GaAs QWs.³ Obviously, the BX time evolution in our GaN QW does not support the equilibrium condition. At the same time, assuming that the biexciton will continuously form from excitons with a formation probability proportional to n_x^2 , the BX rise time would be given by half the exciton decay time (i.e., ≈ 200 ps, in our case), which is much longer than the experimental findings (i.e., ≈ 35 ps). This means that the BX formation only occurs during the early stage of the exciton recombination kinetics.

In order to assess the interplay between the biexciton formation and the exciton recombination kinetics, we performed TR-PL measurements under resonant excitation. The image of the TR-PL, as measured by the streak camera apparatus, is shown in Fig. 4(a) for the detection channel cross polarized with respect to the excitation. The laser energy is tuned at 4 meV above the excitonic PL and appears as a bright spot on the image. The comparison between the time evolutions of the BX (X) emission for resonant and nonresonant excitations is reported in Fig. 4(b) [Fig. 4(c)]. In the case of resonant excitation, we directly photogenerated excitons and faster rise times are observed with respect to the nonresonant excitation (where free carriers are photojected) for both the X and BX bands. In particular, for resonant excitation, the X band shows a fast initial decay which corresponds to the BX rise time. We attribute this fast initial decay (which is of the order of 20 ps) to the early stage exciton recombination before thermalization and stronger localization occur. Let us comment that, despite the very high quality of our sample, in this discussion, we avoided using the term “free excitons” because, strictly speaking, no state is fully delocalized in the presence of disorder. There are no doubts that, within the excitonic distribution of states, levels at lower energies correspond to more localized wavefunc-

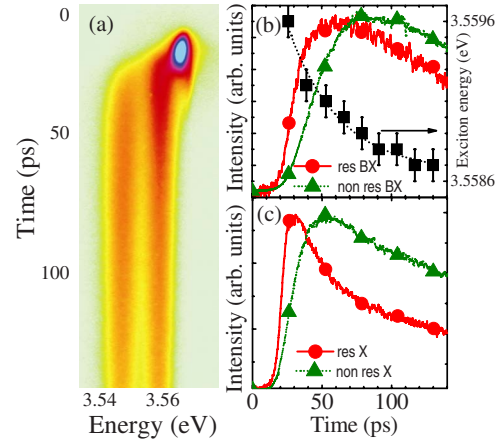


FIG. 4. (Color online) (a) Image of the resonant TR-PL of the 2.6 nm thick GaN/ $\text{Al}_{0.05}\text{Ga}_{0.95}\text{N}$ QW measured at $T=10$ K and at a power density of 20 W/cm^2 under resonant excitation at 348 nm, as measured by the streak camera apparatus. (b) Comparison of the BX time evolution for resonant and non resonant excitation, in linear scale. The energy shift (squares) of the X line under nonresonant excitation is also shown together with an exponential fit (dotted line). (c) Comparison of the X time evolution for resonant and nonresonant excitations in linear scale. The resonant decay corresponds to a detection energy 4 meV below the laser excitation.

tions with respect to levels in the high energy tails, but the distinction between localized and free states (i.e., the concept of mobility edge) has been quite debated in the literature.¹⁶ By resonant excitation, we directly photogenerated excitons which undergo radiative recombination in competition with thermalization and acoustic-phonon mediated relaxation into more localized states at lower energies.¹⁷ On the contrary, in the case of nonresonant excitation, the excitonic formation occurs from photogenerated free carriers, possibly also in high energy exciton states, and therefore exciton recombination arises from a different distribution of excitonic states, which also corresponds to a different recombination kinetics, as observed in our samples. The fast initial decay, observed in the case of resonant excitation, cannot be attributed to resonant Rayleigh scattering^{16–18} simply because our excitation is 4 meV above the detected PL. Note that in Fig. 4(a), at the laser energy, we observe a large Rayleigh contribution, dominated by nonresonant elastic scattering, likely due to surface roughness. Finally, the lifetime measured at longer delays nicely corresponds to the one observed for non resonant excitation, denoting that after interacting with acoustic phonons, excitons eventually reach similar distributions, possibly including dark exciton states, for both resonant and nonresonant excitation conditions.

At the same time, we conclude that the biexciton formation only involves excitons within more delocalized states. Once these excitons relax into more localized states, due to structural disorder in the QW plane, the biexciton formation is quenched and the two populations of X and BX decay with their own radiative lifetime. This picture is strongly supported by the fact that the exciton energy shift and the BX rise time after nonresonant excitation [see Figs. 3(b) and 3(c)] occur on very similar time scales. It is well known that

the TR-PL shift indicates that excitons lose progressively their kinetic energy and get increasingly localized. In this respect, a 35 ps decay time is found for the X energy shift, which nicely corresponds to the BX rise time under nonresonant excitation. Note also that the dynamical PL shift (less than 1 meV) is, as it applies in our case, only a fraction of the measured Stokes shift between PL and PLE spectra.¹⁹ Another confirmation of our picture arises from the very similar decay time of the exciton band for different excitation powers (not shown here), from values where the BX recombination is very weak to the highest excitation. This means that the biexciton formation involves only exciton states which are not populated at long delays.

Hence, the uncoupled recombination dynamics of X and BX in GaN QWs, associated with the small BX ionization rate, allow us to extract the emission lifetime of the BX, which is not accessible in GaAs QWs due to efficient thermalization processes. From an exponential fit of the data, we obtain 210 and 140 ps for the decay times of the X and BX bands, respectively. Theoretically, in quasi-two-dimensional systems, the giant oscillator strength model gives fairly comparable radiative decay rates for excitons and biexcitons,²⁰ while the bipolariton model²¹ predicts a very fast decay of biexcitons into interface polaritons. Experimentally, in GaAs QWs, the TR-PL only reflects the thermal equilibrium³ and four wave mixing experiments show a BX radiative rate which is only slightly larger than the exciton radiative rate.^{6,22} In this respect, the present data would also support the first model, likely due to the fact that the recombination occurs from localized states.

In conclusion, we have shown the presence of biexciton recombination in high quality GaN/AlGaIn single QWs. The

observed large biexciton binding energy inhibits the BX ionization during its lifetime, allowing us to elucidate its radiative kinetics. We have also demonstrated that GaN QWs have reached an optical quality equivalent to that of GaAs based nanostructures, allowing us to study the excitonic and biexcitonic formations and recombinations. The increasing biexciton binding energy with increasing Al content in the barriers, which agrees with the findings in AlGaIn epilayers,²³ can make possible the investigation of biexciton physics above liquid nitrogen temperature (which is also of interest for fundamental physics and applications). These findings also appear very promising in view of realizing more efficient optoelectronic devices, as well as for fundamental studies of the electron-hole correlations in GaN based nanoscale systems. As an example, we point out that owing to their enhanced radiative properties (short radiative lifetime, nearly homogeneous broadening), such high quality QWs should reveal particularly suitable for investigating the strong exciton-photon coupling regime and the related properties of high occupancy coherent polariton states in nitride-based QW microcavities at cryogenic temperatures and above.²⁴

ACKNOWLEDGMENTS

F.S. acknowledges financial support from European Contract No. MRTN-CT-2003-503677. This work was supported by the Italian PRIN-MIUR Contract No. 2005094020 and the NCCR Quantum Photonics (NCCR QP), research instrument of the Swiss National Science Foundation (SNSF). N.G. and R.B. are indebted to the Sandoz Family Foundation for its financial support.

¹D. J. Lovering, R. T. Phillips, G. J. Denton, and G. W. Smith, *Phys. Rev. Lett.* **68**, 1880 (1992).

²R. T. Phillips, D. J. Lovering, G. J. Denton, and G. W. Smith, *Phys. Rev. B* **45**, 4308 (1992).

³J. C. Kim, D. R. Wake, and J. P. Wolfe, *Phys. Rev. B* **50**, 15099 (1994).

⁴F. Kreller, M. Lowisch, J. Puls, and F. Henneberger, *Phys. Rev. Lett.* **75**, 2420 (1995).

⁵Y. Yamada, T. Mishina, Y. Masumoto, Y. Kawakami, S. Yamaguchi, K. Ichino, S. Fujita, S. Fujita, and T. Taguchi, *Superlattices Microstruct.* **15**, 33 (1994).

⁶J. Puls, V. V. Rossin, F. Kreller, H. J. Wunsche, S. Renisch, N. Hoffmann, M. Rabe, and F. Henneberger, *J. Cryst. Growth* **159**, 784 (1996).

⁷P. Bigenwald, A. Kavokin, B. Gil, and P. Lefebvre, *Phys. Rev. B* **61**, 15621 (2000).

⁸S. Nakamura, G. Fasol, and S. J. Pearton, *The Blue Laser Diode: The Complete Story*, 2nd ed. (Springer, Berlin, 2000).

⁹S. F. Chichibu, A. Uedono, T. Onuma, B. A. Haskell, A. Chakraborty, T. Koyama, P. T. Fini, S. Keller, S. P. Denbaars, J. S. Speck, U. K. Mishra, S. Nakamura, S. Yamaguchi, S. Kamiyama, H. Amano, I. Akasaki, J. Han, and T. Sota, *Nat. Mater.* **5**, 810 (2006).

¹⁰S. F. Chichibu, A. Uedono, T. Onuma, T. Sota, B. A. Haskell, S. P. DenBaars, J. S. Speck, and S. Nakamura, *Appl. Phys. Lett.* **86**, 021914 (2005).

¹¹H. Teisseyre, C. Skierbiszewski, B. Lucznik, G. Kamler, A. Feduniewicz, M. Siekacz, T. Suski, P. Perlin, I. Grzegory, and S. Porowski, *Appl. Phys. Lett.* **86**, 162112 (2005).

¹²A. Morel, P. Lefebvre, S. Kalliakos, T. Talierno, T. Bretagnon, and B. Gil, *Phys. Rev. B* **68**, 045331 (2003).

¹³E. Feltin, D. Simeonov, J.-F. Carlin, R. Butté, and N. Grandjean, *Appl. Phys. Lett.* **90**, 021905 (2007).

¹⁴W. Langbein and J. M. Hvam, *Phys. Rev. B* **59**, 15405 (1999).

¹⁵V. Fiorentini, F. Bernardini, F. DellaSala, A. DiCarlo, and P. Lugli, *Phys. Rev. B* **60**, 8849 (1999).

¹⁶R. Zimmermann, E. Runge, and V. Savona, in *Theory of Resonant Secondary Emission: Rayleigh Scattering Versus Luminescence, Quantum Coherence, Correlation, and Decoherence in Semiconductor Nanostructures*, edited by T. Takagahara (Academic, New York, 2003), p. 89.

¹⁷G. Kocherscheidt, W. Langbein, U. Woggon, V. Savona, R. Zimmermann, D. Reuter, and A. D. Wieck, *Phys. Rev. B* **68**, 085207 (2003).

¹⁸M. Gurioli, F. Bogani, S. Ceccherini, and M. Colocci, *Phys. Rev. Lett.* **78**, 3205 (1997).

- ¹⁹Y. Masumoto, S. Shionoya, and H. Kawaguchi, *Phys. Rev. B* **29**, 2324 (1984).
- ²⁰D. S. Citrin, *Phys. Rev. B* **50**, 17655 (1994).
- ²¹A. L. Ivanov, H. Haug, and L. V. Keldysh, *Phys. Rep.* **296**, 237 (1998).
- ²²W. Langbein and J. M. Hvam, *Phys. Rev. B* **61**, 1692 (2000).
- ²³Y. Yamada, Y. Ueki, K. Nakamura, T. Taguchi, Y. Kawaguchi, A. Ishibashi, and T. Yokogawa, *Appl. Phys. Lett.* **84**, 2082 (2004).
- ²⁴S. Christopoulos, G. Baldassarri Höger von Högersthal, A. J. D. Grundy, P. G. Lagoudakis, A. V. Kavokin, J. J. Baumberg, G. Christmann, R. Butté, E. Feltin, J.-F. Carlin, and N. Grandjean, *Phys. Rev. Lett.* **98**, 126405 (2007).